Involvement of multiple intracellular release channels in calcium sparks of skeletal muscle

A. González*, W. G. Kirsch*, N. Shirokova*, G. Pizarro†, G. Brum†, I. N. Pessah‡, M. D. Stern§, H. Cheng§, and E. Ríos*¶

*Department of Molecular Biophysics and Physiology, Rush University, 1750 West Harrison Street, Chicago, IL 60612; †Departamento de Biofísica, Facultad de Medicina, G. Flores 2125, Montevideo, Uruguay; §Laboratory of Cardiovascular Science, Gerontology Research Center, National Institute on Aging, National Institutes of Health, 5600 Nathan Shock Drive, Baltimore, MD 21224; and ‡Department of Molecular Biosciences, School of Veterinary Medicine, University of California, Davis, CA 95616

Communicated by Clara Franzini-Armstrong, University of Pennsylvania School of Medicine, Philadelphia, PA, February 8, 2000 (received for review June 30, 1999)

In many types of muscle, intracellular Ca^{2+} release for contraction consists of brief Ca^{2+} sparks. Whether these result from the opening of one or many channels in the sarcoplasmic reticulum is not known. Examining massive numbers of sparks from frog skeletal muscle and evaluating their Ca^{2+} release current, we provide evidence that they are generated by multiple channels. A mode is demonstrated in the distribution of spark rise times in the presence of the channel activator caffeine. This finding contradicts expectations for single channels evolving reversibly, but not for channels in a group, which collectively could give rise to a stereotyped spark. The release channel agonists imperatoxin A, ryanodine, and bastadin 10 elicit fluorescence events that start with a spark, then decay to steady levels roughly proportional to the unitary conductances of 35%, 50%, and 100% that the agonists, respectively, promote in bilayer experiments. This correspondence indicates that the steady phase is produced by one open channel. Calculated Ca^{2+} release current decays 10- to 20-fold from spark to steady phase, which requires that six or more channels be open during the spark.

excitation-contraction coupling | sarcoplasmic reticulum | ryanodine receptors | caffeine | bastadin

As an intracellular messenger, Ca^{2+} participates in a wide range of processes (1). In muscle, action potentials in the plasma membrane and transverse tubules cause Ca channels of the sarcoplasmic reticulum to open. The ensuing Ca^{2+} release initiates contraction. A portion of this release occurs by superposition of brief local events, which under fluorescence monitoring appear as "Ca^{2+} sparks" in cardiac (2, 3), skeletal (4, 5), and smooth muscle (6). Sparks are fundamental in health and disease (7), but their mechanism, especially whether one or many channels are involved in the spark generator or "release unit," remains unclear (8–10). Answering this question, which pervades the field since its inception (2), will help understand how the channels are coaxed by their agonists (Ca, membrane voltage; reviewed in refs. 11 and 12) and restrained by their antagonists (Ca, Mg) to shape these events.

Here we improve a technique for detection of massive numbers of sparks (13) and apply it, together with a method to evaluate the Ca^{2+} release current underlying a spark (14), to events modified by drugs that stabilize open channel states. Caffeine (15) allows us to characterize the distribution of open times of the spark-generating sources. To gauge the releasing ability of a single channel we then analyze the events elicited by three drugs that induce long-lived states. Imperatoxin A (Iptx; refs. 8 and 16) and ryanodine (Ry; refs. 18 and 19) demonstrate what a channel can do in a subconductance state; bastadin 10 (B10; ref. 20) reversibly stabilizes the fully open state. By comparing open time and release flux of sparks with those of the drug-induced events, we evaluate approximately the relative numbers of channels involved.

Materials and Methods

Experiments were carried out at 17°C in cut skeletal muscle fibers from *Rana pipiens* semitendinosus muscle, stretched at 3–3.5 μm/sarcomere, either voltage-clamped in a two-Vaseline gap chamber or permeabilized and immersed in internal solution, on an inverted microscope. Adult frogs anaesthetized in 15% ethanol were killed by pithing. The external solution contained 10 mM $Ca(CH_3SO_3)_2$, 130 mM tetraethylammonium-CH_3SO_3, 5 mM Tris maleate, 1 mM 3,4 diaminopyridine, and 1 μM tetrodotoxin. The internal solution contained 110 mM Cs-glutamate, 1 mM EGTA, 5 mM glucose, 5 mM Mg-ATP, 5 mM phosphocreatine, 10 mM Hepes, 0.2 mM fluo-3, with 100 nM free [Ca^{2+}] and 1.8 mM [Mg^{2+}]. For permeabilized cells the internal solution contained 0.05 mM fluo-3 and 0.34 mM [Mg^{2+}] and included 4% 10-kDa dextran. Solutions were adjusted to pH 7 and 270 mosmol/kg. The scanning microscope (MRC 1000, Bio-Rad) was in fluo-3 configuration (14) using a 40×, 1.2 numerical aperture water immersion objective (Zeiss). Images shown are of fluorescence determined at 2-ms intervals (4.3 ms in toxin experiments) along a parallel to the fiber axis. Fluorescence $F(x,t)$ is presented normalized to its average $F_0(x)$ before the voltage pulse. Sparks are located on a spatially filtered version of the image as described in ref. 13. Parameters measured on the unfiltered image for every event include: amplitude (peak minus local average before the event), spatial width of the region exceeding half amplitude at the time of peak, and rise time (between 0.1 and peak, on a spline interpolate). Rise times were not corrected for distortion because of off-focus imaging, noting that temporal magnitudes (rise time and duration) are much less subject to such errors than amplitude or spatial width (e.g., ref. 21).

Ca^{2+} release flux and current were calculated as described (14) by first deriving $[Ca^{2+}]_i$ from the measured fluorescence, then calculating numerically the flux of binding and removal of Ca^{2+} onto cellular sites, at consensus concentrations and binding parameter values (listed in table 1 of ref. 14). Sparks were simulated as the result of Ca^{2+} release from a source of known intensity and open time into a homogeneous medium with fixed and diffusible Ca^{2+} binding sites, mimicking the cytoplasm (14). For tests of the detection procedure, line-scan images were simulated by adding resting fluorescence, noise, and sparks in random positions to an array with the dimensions of an image. So that rise times would not be correlated with amplitude (a property noted by Lacampagne *et al.* in ref. 23), sparks were first

Abbreviations: Ry, ryanodine; B10, bastadin 10; Iptx, imperatoxin A.

¶To whom reprint requests should be addressed at: Department of Molecular Biophysics and Physiology, Rush University, 1750 West Harrison Street, Suite 1279 JS, Chicago, IL 60612. E-mail: erios@rush.edu.

The publication costs of this article were defrayed in part by page charge payment. This article must therefore be hereby marked "*advertisement*" in accordance with 18 U.S.C. §1734 solely to indicate this fact.

Article published online before print: *Proc. Natl. Acad. Sci. USA*, 10.1073/pnas.070056497. Article and publication date are at www.pnas.org/cgi/doi/10.1073/pnas.070056497

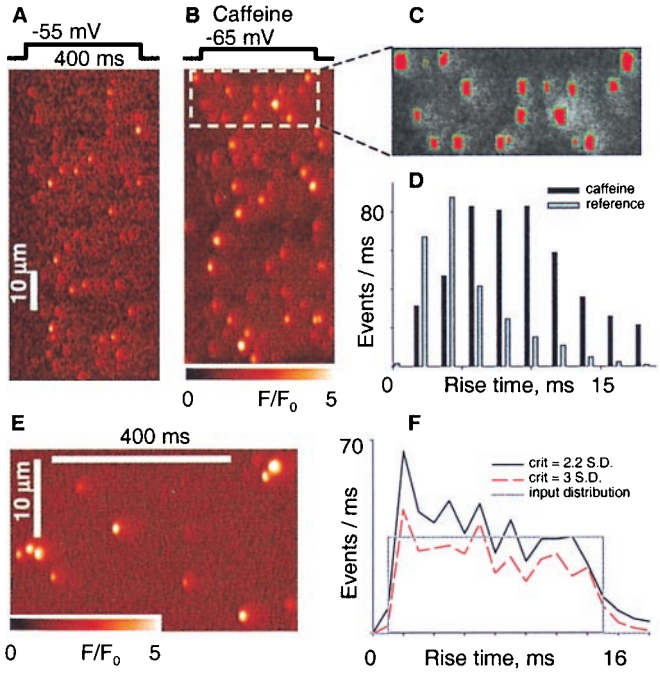

Fig. 1. The distribution of spark rise times. (*A*) Line-scan image of a fiber held at −90 mV and pulsed to −55 mV as indicated. Fluorescence *F* normalized to the initial fluorescence F_0. (*B*) The same fiber as in *A* exposed to 1 mM caffeine externally. (*C*) The detector's performance: rectangles mark the sides of regions, in red, where F/F_0 exceeded 3 SD of the fluorescence in neighboring, nonspark areas (12). (*D*) Histograms of rise times for 514 events in reference and 938 in caffeine. Cell identifier 0315a. (*E*) Portion of an image generated placing simulated sparks and Gaussian noise at random positions in an array dimensioned as a line-scan image. Sparks were simulated with source openings lasting between 1 and 15 ms, and seven of each were placed in every image. Sparks were scaled to reproduce off-focus effects and other properties of experimental images (details in *Materials and Methods*). (*F*) Rise time histograms of events detected in five simulated images using different threshold criteria. In gray, input distribution, constant between 1 and 15 ms.

scaled to the same amplitude A. Subsequently, sparks (of the same rise time) were rescaled between A and $A/10$, so that the distribution of amplitudes (a) would be proportional to $1/a$, as prescribed by Izu *et al.* (24) to account for off-focus scanning. Signal mass was calculated by volume integration of normalized fluorescence, assumed to be spherically symmetric.

Results

Fig. 1 shows line-scan images, collected from a cell held by voltage clamp at −90 mV and depolarized as indicated. Caffeine (1 mM) (Fig. 1*B*) rapidly and reversibly increased spark size and numbers. In multiple images from the same cell large numbers of sparks were located by an automatic procedure (13) that also tabulates their amplitude, spatial width, and rise time. Fig. 1*C* shows a graphic output of the automatic locator: red marks the area where a threshold criterion is met (increase in relative fluorescence over a global mean > 3 SD of the neighboring regions without sparks).

Fig. 1*D* shows the histograms of rise times of events from 17 images. In reference the distribution of rise times was generally monotonic, as expected if sparks result from reversible openings of single Markovian channels (25). By contrast, in four experiments at 1 mM caffeine and six at 0.5 mM there was a broad mode, at between 6 and 10 ms.

Multiple tests confirmed the dearth of brief events in caffeine. If the mode in Fig. 1*D* was caused by missed events, it should depend on the detector's sensitivity. Lowering the detection threshold induced a frequency peak at low rise times (consisting in false detections), without changing the mode at higher rise times (not shown). Tests using simulated sparks (Fig. 1 *E* and *F*) showed that the method did not produce a spurious mode when operating on a set of events with a flat distribution of rise times.

Although the observation was obvious in cells modified by caffeine, in three of 13 experiments in reference there was a clear mode at 6 ms. The modal distribution of open times is probably a pre-existing property, more easily demonstrated under caffeine. This conclusion is in indirect agreement with two recent studies of sparks originating at repetitively firing units, which did not produce low-amplitude events in the proportion expected from exponentially distributed open times (26, 27). Therefore, sparks cannot be produced by single Markovian release channels gating reversibly.

While favoring channel groups as sources of sparks, a stereotyped open time does not rule out single channels, which could be gating irreversibly, drawing energy from the $[Ca^{2+}]$ gradient between sarcoplasmic reticulum and cytoplasm (9). Independent evidence in favor of multiple channels was obtained by using three other drugs that stabilize open states. Iptx opens the channel to a substate of 1/3 conductance in bilayer experiments (16). Low concentrations of the toxin induce long-lasting fluorescence events (A. Shtifman, C. W. Ward, H. H. Valdivia, and M. F. Schneider, personal communication; ref. 8). Like most, those shown in Fig. 2*A* are immediately preceded by brief "starter" events. Fig. 2 *B* and *C* shows temporal and spatial profiles of the starter and long event at the top. Table 1 lists morphology parameters of 75 long events and their starters, together with those of 1,625 sparks detected in the same experiments.

In bilayer experiments, the toxin prefers to bind to fully open channels (16). Therefore, if channels worked alone to produce sparks a starter would be expected, reflecting the channel's passage through the fully open state before toxin binding. This view yields two predictions: (*A*) the rise time of starters ought to be less than that of sparks, (simply because channel openings are cut short by toxin binding), and their amplitude ought to be correspondingly reduced; and (*B*) the release flux of steady and starter events should be in the ratio of subconductance and full conductance.

We developed an expression for the expected dwell time τ_{Tx} of an open state (originally of dwell time τ) when interrupted by binding of a toxin Tx. Let $P(t)$ be the probability that the channel remains open at time t. The mean open duration then is given by:

$$\tau_{eff} = -\int_0^\infty \frac{dp}{dt} t \, dt = \int_0^\infty P(t) \, dt. \qquad [1]$$

Let $P_0(t)$ represent probability in the absence of the toxin, and $K[Tx]$ the binding rate of toxin in any open state, then

$$P(t) = P_0(t) \, e^{-tK[Tx]} \qquad [2]$$

which can be used in Eq. **1** to calculate τ_{eff}.

If attention is confined to those openings that are terminated by toxin binding (starters in the single-channel hypothesis of sparks), the rate of such terminations is clearly $P(t)K[Tx]$, which gives, for their mean open duration:

$$\tau_{Tx} = \frac{\int_0^\infty t \, P_0(t) \, e^{-tK[Tx]} \, dt}{\int_0^\infty P_0(t) \, e^{-tK[Tx]} \, dt}. \qquad [3]$$

The results of Eqs. **2** and **3** depend on the shape of $P_0(t)$. We evaluated Eq. **3** analytically, for three forms of $P_0(t)$ (an exponential of time constant τ, a constant up to time 2τ, and a distribution concentrated at τ) and numerically, for the distri-

PHYSIOLOGY

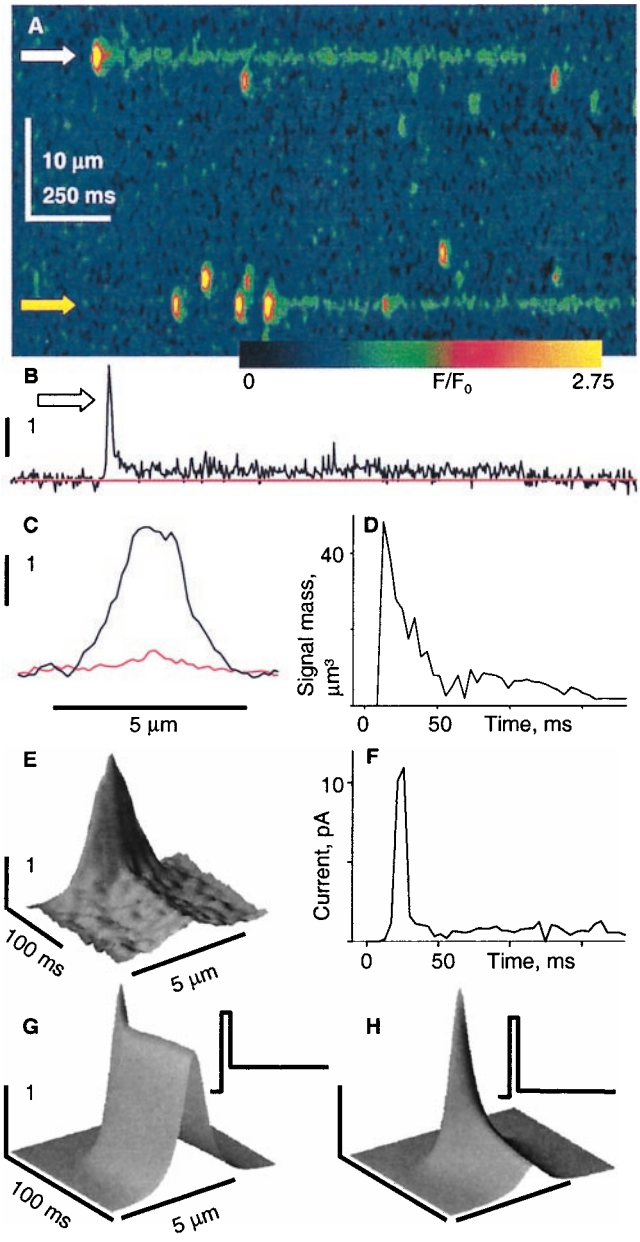

Fig. 2. Sparks and Iptx-induced openings. (*A*) Image of a permeabilized cell, immersed in solution with 100 nM Iptx (a gift from H. Valdivia, University of Wisconsin, Madison). (*B*) Temporal profile of F/F_0 at white arrow. (*C*) Spatial profile of F/F_0 at the peak of the starter event and its average (red) during the long event that follows. Identifier 0416b. (*D*) Time course of signal mass, volume integral of the normalized fluorescence increase in a 6-μm radius. (*E*) An average of nine long events selected by their large amplitude, from two cells in which the resting fluorescence was similar (0416b, 0423a). F/F_0, time and space represented by coordinates *z*, *x*, and *y*, respectively. (*F*) Release current, calculated from the average event in *C* (14, 30). (*G*) Simulated fluorescence event for a Ca^{2+} source of initial current 10 pA, lasting 6 ms, followed by a steady current of 3.3 pA (*Inset*). (*H*) Simulation where the opening at 10 pA is followed by a steady 0.5-pA current. The source diameter was 0.05 μm. Details and parameter values of the simulation were as described in ref. 14.

butions observed experimentally, with results that were less than τ in every case.

Hence if starters were caused by toxin-interrupted openings of single channels, their expected rise time would be less than that in regular sparks and their amplitude would be correspondingly reduced.

Against prediction *A*, the average amplitude of starters (Table 1) was significantly greater than that of sparks, whereas their spatial width and duration were not different. Starters are thus similar to sparks; if toxin binding occurs at some point during their development, it does not curtail them in any visible way. That starters are greater than the average spark is understandable if both require multiple channels. Indeed, for involving more open channels and thereby presenting a bigger toxin target larger sparks would be expected to lead more frequently to a long toxin-induced event.

A one-channel explanation for starters is that the toxin might stabilize the full open state (making it longer lasting), then the substate. Although possible, this would require a non-Markovian channel, because the sequence always proceeds from starters to long events.

To test prediction *B* starter and steady release flux were compared. The time course of signal mass (29) during the event in Fig. 2 *B* and *C*, plotted in Fig. 2*D*, shows a 7.7-fold reduction from the initial peak (7.48 ± 1.14 for 66 events). Because the large signal mass of the starter is generated during the brief rise time period, the ratio of release flux or current between starter and steady phases must be greater than the corresponding ratio of signal masses. This point is made quantitative by calculating release flux and current from first principles (as described in refs. 14 and 30). Because the method relies on assumptions for binding and diffusion parameters of the many Ca^{2+} binding molecules, it is best as a comparison tool, especially for sources located, as in this case, essentially in the same place, presumably facing the same concentrations of ligands.

To reduce noise and have a more representative result, the method was applied to the average in Fig. 2*E* of nine large toxin-induced events. The resulting release current (Fig. 2*F*) peaks at 11.3 pA and then decays to a steady value of 0.68 pA (a 16.6 peak/steady ratio). The calculation then was applied with two widely different sets of parameter values, devised so that peak current changed by a factor of 4, but the ratio remained within a 2-fold range (11.5 to 24.1). If the steady release corresponded to a single channel in a 35% conductance state, then a 16.6-fold greater peak would require six fully open channels. (Because the low temporal resolution in data acquisition results in an underestimate of peak but not of steady release rate, the number of channels is probably greater.)

The above calculation of release flux, working "backward" from the fluorescence increase, was checked with "forward" calculations—simulations, like those in Fig. 1*E*—that start from the current. Fig. 2 *G* and *H* shows the fluorescence for a source of two stages (*Inset*), a "full open" current lasting 6 ms, then a lower steady level. The steady level was either 1/3 of the early current (Fig. 2*G*) or 1/20 (Fig. 2*H*). Clearly, two very different stages of release flux, in a ratio of 20:1 or greater, are necessary to reproduce the toxin-induced signal in Fig. 2*E*.

In addition to starters there are often spark-like events overlapping the long toxin-induced opening (Fig. 3 *A* and *B*). Given the low overall activity in these examples, it is highly unlikely that the sparks originated anywhere but in the toxin-bound unit. The sparks in Fig. 3*A* demonstrate, given their large and nearly constant size, that the termination of the starter is not caused by local depletion. The variable amplitudes of the sparks in Fig. 3*B*, which in this and other examples were not correlated with their rise time, are best explained as the consequence of activation of variable numbers of channels.

If multiple channels opened during a spark, this should occasionally allow more than one channel to bind toxin. Regardless of mechanism, the coexistence of 66 long events (with starters) and 1,625 regular sparks reflects a probability of 1/24 that a spark will lead to toxin binding. Hence *P* of two molecules binding independently to one spark generator would be one in 588 sparks (three in 1,625). Indeed, three of the long events

Table 1. Properties of agonist-induced events and sparks

Events	Number		Amplitude		FWHM, μm		Rise time, ms
	With starter	Without starter	Peak	Steady	Peak	Steady	
Toxin-induced	66	9	2.48 (0.13)	0.30 (0.02)	1.35 (0.07)	1.49 (0.06)	8.8 (0.55)
Sparks	1,625		1.69 (0.02)		1.40 (0.01)		8.7 (0.1)
Ry-induced	84	12	2.35 (0.10)	0.41 (0.04)	1.19 (0.07)	1.61 (0.09)	6.3 (0.98)
Sparks	963		1.85 (0.04)		1.35 (0.03)		6.9 (0.19)
B10-induced	74	17	2.27 (0.08)	0.59 (0.03)	1.33 (0.06)	1.86 (0.06)	6.6 (0.65)
Sparks	3,489		1.73 (0.01)		1.61 (0.01)		5.1 (0.05)

Events collected from eight experiments with Iptx, four with Ry, and three with B10. Parameters of events without starters, induced by B10 or Ry, were not significantly different from the corresponding ones for the steady phase of events with starters elicited by the same agonist. The entries under "Sparks" always correspond to events collected in the same fibers. The amplitude of the sparks listed was at least 1.0, i.e., the amplitude of the smallest starter included in the table. FWHM, spatial width of the region exceeding half amplitude at the time of peak. Numbers in parentheses are SEM.

observed decayed in two nearly equal steps. Fig. 3*C* shows an example. In this experiment the frequency of long events was $\approx 10^{-2}$ per image per Z disk (nine images). Hence, P of two independent events in the same Z disk was 10^{-4}, and that of their starting simultaneously (i.e., within the same one or two line scans) was $<10^{-6}$. Therefore, the double-step event could not have originated in two independent units and instead must have involved two channels in the same unit. This constitutes direct evidence of the presence of multiple channels in the same spark-producing unit.

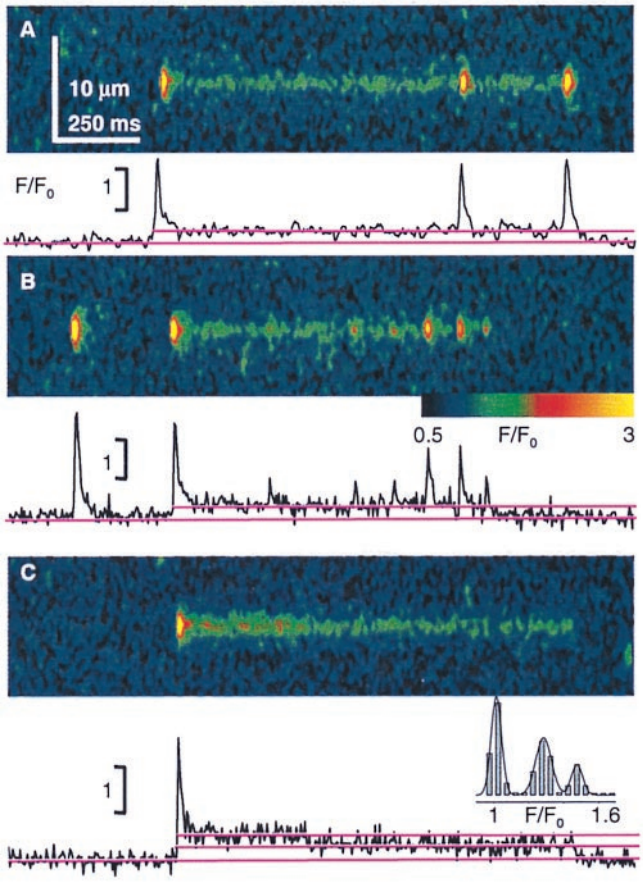

Fig. 3. Multiple channels within the same release unit. The graphs plot F/F_0 averaged over five spatial pixels (0.7 μm) centered at the starter. (*A* and *B*) Toxin-induced events with multiple sparks from the same unit. (*A*) Repeated large sparks indicate that Ca^{2+} depletion is not a factor in their termination. (*B*) Sparks of variable amplitudes, coming from the same unit. (*C*) Example toxin event that decays in two steps of similar amplitude. (*Inset*) Amplitude histogram from F/F_0 after one smoothing step, with Gaussian fit of means 1.01, 1.28, and 1.49. Identifiers were 0423b (*A* and *C*) and 0414a (*B*).

Occasionally long event and starter occurred at different locations. An example is at the yellow arrow in Fig. 2*A*: the long event is visibly displaced from the center of its starter and the sparks that preceded it in the same disk. Its center of mass was shifted 0.133 μm from that of its starter, suggesting an extensive release unit. Significance of the spatial shift was established at a $P = 0.05$ by a t test of the difference between the average placement of the centers of mass of the sparks, and that of the centers of 28 equally weighted regions automatically located within the long event.

Iptx conceivably could take a single channel through a multistep ladder of subconductances on the way to closure, thereby explaining the two-step events. This remote possibility (it would require a channel with non-Markovian properties, as the sequence: full open > first step > second step > closed was never observed to occur in reverse) was tested by using other ligands with different properties. Ry is perhaps the best understood agonist of its receptor. At submicromolar concentrations it induces a long-lived state of ≈50% conductance, by high affinity binding to a site or sites most available when the channel is open (31, 32). Representative images obtained within 30 min of exposure to 50 nM Ry (Fig. 4) reveal a generally increased frequency of sparks, plus stable, long-lasting fluorescence events, very similar to those with Iptx. Most events have a starter, which, as listed in Table 1, is slightly greater than the average spark in the same experiments. The tabulated averages indicate that the starters were not different from those in Iptx but the steady fluorescence increase, at 0.41, was significantly greater. The ratio of average peak (starter) to steady fluorescence increase was 5.7. The release current, calculated as described for Iptx on an average of 14 events, was 10.0 pA and 0.63 pA, respectively, for a ratio of 16. Fig. 4*B* documents the observation, in four cells, that amplitude and width of starters, but not of steady events, decreased after 30–60 min of exposure to 50 nM Ry, while the frequency of sparks diminished and that of the steady events (two are shown) appeared to increase. These late changes are avoided in Table 1, by pooling data from the initial 30 min of exposure only. Fig. 4*C* shows an event decaying in two steps.

We also tested B10, a sponge extract component whose mechanism has been elucidated in detail at the single-channel level (20). B10 provides a crucial term of comparison because: (*i*) in bilayers its actions are fully reversible, (*ii*) it stabilizes the full open state of the channel, increasing P_o to near unity (at 5 μM), (*iii*) the unitary conductance is not altered, (*iv*) it has no subconductance states, and (*v*) its effector site is distinct from the Ry sites.

PHYSIOLOGY

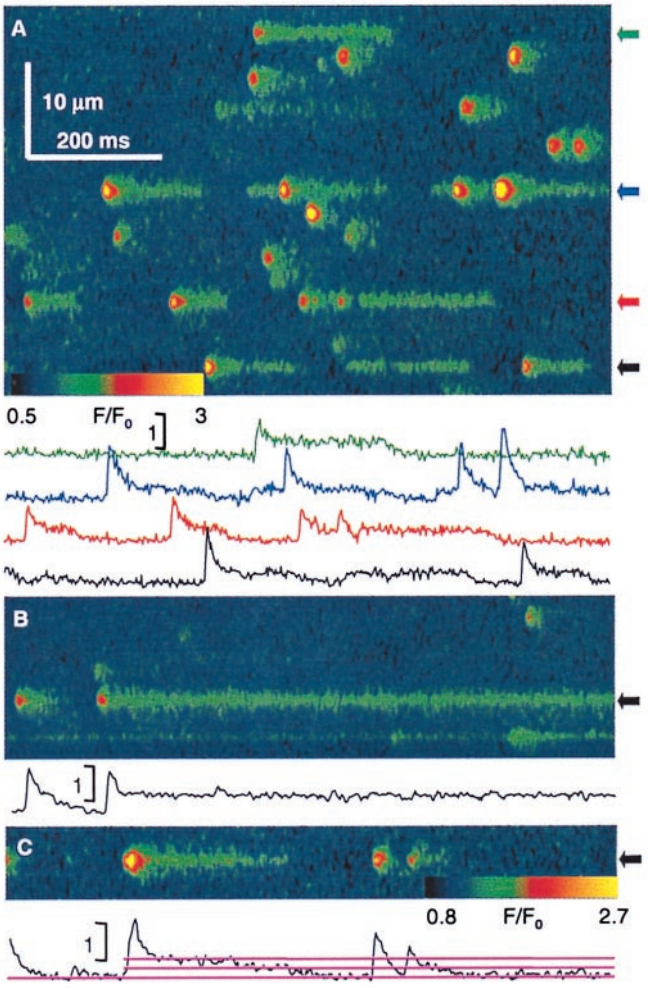

Fig. 4. Sparks and long openings induced by Ry. (*A*) Normalized line-scan image in a permeabilized fiber immersed 15 min in internal solution with 50 nM Ry. Traces plot F/F_0 averaged over a 0.7 μm-wide region. Note the long openings, beginning with a starter or, occasionally, without one (black). (*B*) After ≈50-min exposure frequency of sparks and amplitude of starters decreases. Very long-lasting events are present. (*C*) Example event that decays in two steps. Identifiers were 1012a66, 1015a60, and 1025a112.

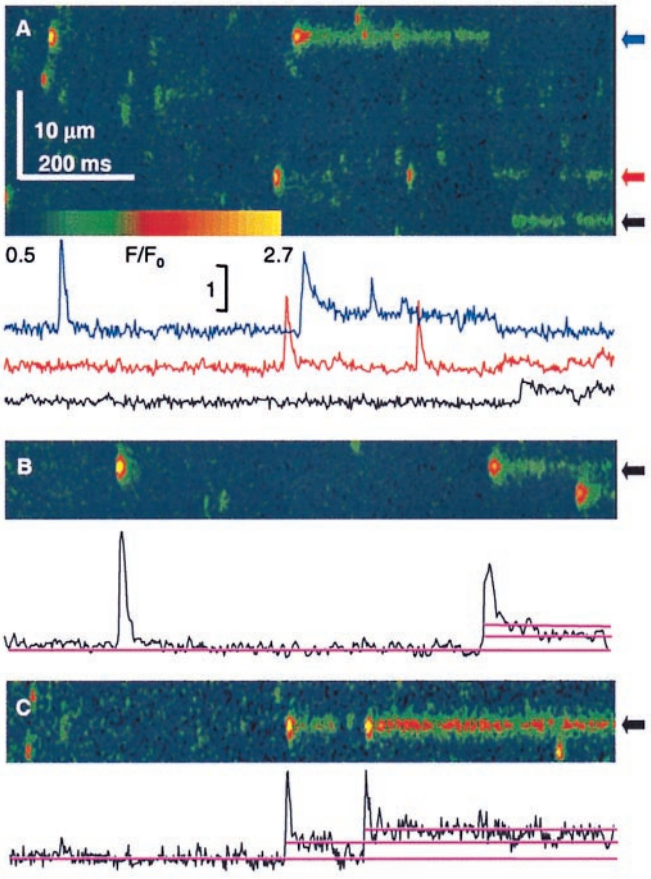

Fig. 5. Events in the presence of B10. Line-scan images (F/F_0) in permeabilized cells in 10 μM B10. The long-lasting openings are qualitatively similar to those induced by Iptx or Ry. Most have a starter, but there are events without one (red). Some have superimposed sparks (blue). Two-step decay (*B*) and double-amplitude events (*C*) may be observed. Identifiers were 0617c53, 0617c91, and 0617b50.

When applied to permeabilized fibers, 10 μM B10 significantly increased event frequency, like Ry, suggesting that both drugs may bind to closed channels. As represented in Fig. 5, it also elicited long events, most of which had a starter and a steady phase. They could have superimposed multiple sparks of different amplitudes (Fig. 5*A*). Two-stage decays were found (Fig. 5*B*), as well as double-size events (Fig. 5*C*), again implying a degree of drug preference for open channels. As listed in Table 1, the starter's characteristics were similar to those of sparks in the same experiments, and the steady fluorescence increase was on average 0.59, significantly greater than Iptx- or Ry-induced events. The release currents calculated on an average of 17 events were 7.4 and 0.78 pA at peak and steady levels, respectively, for a ratio of 9.5.

Discussion

Whether sparks are produced by single or multiple channels matters for elucidating the mechanisms of control at work in excitation-contraction coupling (8–10). Arguments for a multichannel origin include the large flux calculated for Ca^{2+} sparks, which is inconsistent with measurements of unitary Ca^{2+} currents in bilayers (33), and the complex "quantal" properties of the initial peak of release flux elicited by clamp depolarization (34), hardly explicable as the addition of individually determined one-channel contributions. The rapid turn-on and -off of the causative release (21) and the lack of effects of low [Mg^{2+}] on spark amplitude (35) lend credence to the one-channel theory.

In the present work several observations support the multichannel hypothesis. First is the stereotyped rise time of sparks. In theory a channel could have a modal distribution of open times under special conditions (9, 36, 37), but there are exceedingly few experimental examples of such distributions (28).

A more direct demonstration is in the evolution of release flux in openings induced by three drugs of diverse structures and mechanisms. Most long-lasting drug events had an early starter. In principle, this is consistent with a single channel that briefly opens fully, then is locked by the drug in a substate. This explanation can be rejected on quantitative and qualitative grounds. The starters that initiate most drug events require a flux 10–20 times greater than that during the steady portion of the event. Moreover, B10, a drug that does not promote substates (20), induced fluorescence events qualitatively similar to those seen with the other drugs. The sole differences were in the levels of steady fluorescence increase, which were roughly consistent with the conductances promoted in bilayers (35%, 50%, and 100%, respectively for Iptx, Ry, and B10).

An additional argument is provided by the somewhat larger size of starters relative to sparks, contrary to the expectation if

starters (and sparks) corresponded to a channel going through a fully open state, which in the case of starters is interrupted by the toxin. Yet another is the existence of sparks of many different sizes, coming from the same release unit (Figs. 2*A* and 4*A*), which must have been produced by release events of different current intensity because there was not a correlative variation in rise time.

The most direct evidence of multiple channels in the same release unit is the existence of drug-induced events decaying in two steps of almost equal amplitude. This requires two channels because the reverse transition, a two-step rise, was never observed, under any drug, and also because two-step events occurred with B10, which in bilayers does not induce substates (20). Additionally, the step size (similar to the average size of one-step events) is consistent with the two-channel explanation, as is the frequency of the Iptx-induced two-step events. Finally, the occasional spatial displacement of long events with respect to the center of the starter suggests that sources may extend $\approx 0.15\ \mu$m in a direction parallel to the fiber axis. Taken together, these observations constitute evidence that Ca^{2+} sparks in the present experiments result from opening of several (six or more) channels.

The cohort of channels that underlie a spark could include all or some of the channels in a couplon (38, 39), the excitation-contraction coupling structures on one side of a junctional tranverse tubule-sarcoplasmic reticulum segment (40). In agreement, initial modeling of couplon responses yielded a distribution of open source times with a clear mode (38).

To start Ca^{2+} release, action potentials induce a conformational change in voltage sensors of the transverse tubule membrane. In current skeletal muscle models (5, 22, 38, 41) this directly opens underlying channels, providing Ca^{2+} to trigger other channels that do not contact the sensor. By not having to directly open all channels, such models increase gain and speed, while displaying the stability and rich modulatory behavior observed experimentally (34, 38). The drugs used here appear to exemplify a similar mechanism, where the long event represents the hypothetical voltage-operated opening, whereas the starter reflects the secondary opening of a channel group.

Interestingly, in the initial work with cardiac myocytes (2), the events induced by Ry had small or no starters and therefore were taken to support a single-channel origin of sparks. The present observations suggest instead that the events observed in myocytes may have corresponded to the "late" events reported in the present work, when for unknown reasons, probably related to the multiple time-dependent effects of Ry (31, 32), starters become smaller or disappear altogether.

Scarce (42) or absent (43) in adult mammalian skeletal muscle, sparks are demonstrated best in amphibians, where structural knowledge of the transverse tubule-sarcoplasmic reticulum junction is less complete (40). Therefore, even though the involvement of multiple channels is strongly supported here, their structural location remains to be established. Because Ca^{2+} release during sparks starts and ends abruptly (23), an allosterically connected cluster (17, 44) may be at work. These and other issues must be clarified to base a cellwide picture of Ca^{2+} release on the properties of its channels and their sensors.

A.G. dedicates this work to Prof. Alejandro Illanes. We thank Dr. H. Valdivia for the generous gift of Iptx and advice on its use. This work was supported by grants from the National Institutes of Health to E.R., N.S., and I.N.P. and by intramural research programs of the National Institutes of Health to M.D.S and H.C.

1. Clapham, D. E. (1995) *Cell* **80,** 259–268.
2. Cheng, H., Lederer, W. J. & Cannell, M. B. (1993) *Science* **262,** 740–744.
3. López-López, J. R., Shacklock, P. S., Balke, C. W. & Wier, W. G. (1995) *Science* **268,** 1042–1045.
4. Tsugorka, A., Ríos, E. & Blatter, L. A. (1995) *Science* **269,** 1723–1726.
5. Klein, M. G., Cheng, H., Santana, L. F., Jiang, Y. H., Lederer, W. J. & Schneider, M. F. (1996) *Nature (London)* **379,** 455–458.
6. Nelson, M. T., Cheng, H., Rubart, M., Santana, L. F., Bonev, A. D., Knot, H. J. & Lederer, W. J. (1995) *Science* **270,** 633–637.
7. Gómez, A. M., Valdivia, H. H., Cheng, H., Lederer, M. R., Santana, L. F., Cannell, M. B., McCune, S. A., Altschuld, R. A. & Lederer, W. J. (1997) *Science* **276,** 800–806.
8. Schneider, M. F. (1999) *J. Gen. Physiol.* **113,** 365–372.
9. Shirokova, N., González, A., Kirsch, W. G., Ríos, E., Pizarro, G., Stern, M. D. & Cheng, H. (1999) *J. Gen. Physiol.* **113,** 377–384.
10. Cannell, M. B. & Soeller, C. (1999) *J. Gen. Physiol.* **113,** 373–376.
11. Schneider, M. F. (1994) *Annu. Rev. Physiol.* **56,** 463–484.
12. Meissner, G. (1994) *Annu. Rev. Physiol.* **56,** 485–508.
13. Cheng, H., Song, L. S., Shirokova, N., González, A., Lakatta, E. G., Ríos, E. & Stern, M. D. (1998) *Biophys. J.* **76,** 606–619.
14. Ríos, E., Stern, M. D., Gonzalez, A., Pizarro, G. & Shirokova, N. (1999) *J. Gen. Physiol.* **114,** 31–48.
15. Herrmann-Frank, A., Lüttgau, H.-C. & Stephenson, D. G. (1999) *J. Muscle Res. Cell Motil.* **20,** 223–237.
16. Tripathy, A., Resch, W., Xu, L., Valdivia, H. H. & Meissner, G. (1998) *J. Gen. Physiol.* **111,** 679–690.
17. Stern, M. D., Song, L. S., Cheng, H., Sham, J. S., Yang, H. T., Boheler, K. R. & Rios, E. (1999) *J. Gen. Physiol.* **113,** 469–489.
18. Imagawa, T., Smith, J. S., Coronado, R. & Campbell, K. P. (1987) *J. Biol. Chem.* **262,** 16636–16643.
19. Rousseau, E., Smith, J. S. & Meissner, G. (1987) *Am. J. Physiol.* **253,** C364–C368.
20. Chen, L., Molinski, T. F. & Pessah, I. N. (1999) *J. Biol. Chem.* **274,** 32603–32612.
21. Jiang, Y. H., Klein, M. G. & Schneider, M. F. (1999) *Biophys J.* **77,** 2333–2357.
22. Shirokova, N. & Ríos, E. (1997) *J. Physiol.* **502,** 3–11.
23. Lacampagne, A., Ward, C. W., Klein, M. G. & Schneider, M. F. (1999) *J. Gen. Physiol.* **113,** 187–198.
24. Izu, L. T., Wier, W. G. & Balke, C. W. (1998) *Biophys. J.* **75,** 1144–1162.
25. Colquhoun, D. & Hawkes, A. (1995) in *Single Channel Recording*, eds. Sakmann, B. & Neher, E. (Plenum, New York), pp. 397–482.
26. Klein, M. G., Lacampagne, A. & Schneider, M. F. (1999) *J. Physiol.* **515,** 391–411.
27. Bridge, J. H., Ershler, P. R. & Cannell, M. B. (1999) *J. Physiol* **518,** 469–475.
28. Gration, K. A., Lambert, J. J., Ramsey, R. L., Rand, R. P. & Usherwood, P. N. (1982) *Nature* (*London*) **295,** 599–603.
29. Sun, X. P., Callamaras, N., Marchant, J. S. & Parker, I. (1998) *J. Physiol.* **509,** 67–80.
30. Blatter, L. A., Hüser, J. & Ríos, E. (1997) *Proc. Natl. Acad. Sci. USA* **94,** 4176–4181.
31. Sutko, J. L., Airey, J. A., Welch, W. & Ruest, L. (1997) *Pharmacol. Rev.* **49,** 53–98.
32. Buck, E., Zimanyi, I., Abramson, J. J. & Pessah, I. N. (1992) *J. Biol. Chem.* **267,** 23560–23567.
33. Mejía-Alvarez, R., Kettlun, C., Ríos, E., Stern, M. & Fill, M. (1999) *J. Gen. Physiol.* **113,** 177–186.
34. Pizarro, G., Shirokova, N., Tsugorka, A. & Ríos, E. (1997) *J. Physiol.* **509,** 289–303.
35. Lacampagne, A., Klein, M. G. & Schneider, M. F. (1997) *J. Gen. Physiol.* **111,** 207–224.
36. Schneggenburger, R. & Ascher, P. (1997) *Neuron* **18,** 167–177.
37. Chen, T. & Miller, C. (1996) *J. Gen. Physiol.* **108,** 237–250.
38. Stern, M. D., Pizarro, G. & Ríos, E. (1997) *J. Gen. Physiol.* **110,** 415–440.
39. Franzini-Armstrong, C., Protasi, F. & Ramesh, V. (1999) *Biophys. J.* **77,** 1528–1539.
40. Franzini-Armstrong, C. & Jorgensen, A. O. (1994) *Annu. Rev. Physiol.* **56,** 509–534.
41. Ríos, E. & Pizarro, G. (1988) *News Physiol. Sci.* **3,** 223–227.
42. Conklin, M., Powers, P., Gregg, R. & Coronado, R. (1999) *Biophys. J.* **76,** 657–669.
43. Shirokova, N., García, J. & Ríos, E. (1998) *J. Physiol.* **512,** 377–384.
44. Marx, S. O., Ondrias, K. & Marks, A. R. (1998) *Science* **281,** 818–821.